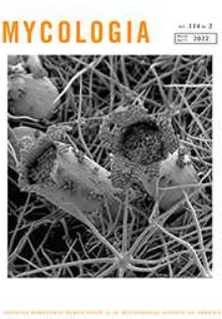

Mycologia

ISSN: (Print) (Online) Journal homepage: https://www.tandfonline.com/loi/umyc20

Darksidea phi, sp. nov., a dark septate root-associated fungus in foundation grasses in North American Great Plains

María-José Romero-Jiménez, Jennifer A. Rudgers, Ari Jumpponen, José Herrera, Miriam Hutchinson, Cheryl Kuske, John Dunbar, Dániel G. Knapp, Gábor M. Kovács & Andrea Porras-Alfaro

To cite this article: María-José Romero-Jiménez, Jennifer A. Rudgers, Ari Jumpponen, José Herrera, Miriam Hutchinson, Cheryl Kuske, John Dunbar, Dániel G. Knapp, Gábor M. Kovács & Andrea Porras-Alfaro (2022) *Darksidea phi*, sp. nov., a dark septate root-associated fungus in foundation grasses in North American Great Plains, Mycologia, 114:2, 254-269, DOI: 10.1080/00275514.2022.2031780

To link to this article: https://doi.org/10.1080/00275514.2022.2031780

MYCOLOGIA
2022, VOL. 114, NO. 2, 254–269
https://doi.org/10.1080/00275514.2022.2031780

Taylor & Francis
Taylor & Francis Group

Darksidea phi, sp. nov., a dark septate root-associated fungus in foundation grasses in North American Great Plains

María-José Romero-Jiménez[a], Jennifer A. Rudgers[b], Ari Jumpponen[c], José Herrera[d], Miriam Hutchinson[e], Cheryl Kuske[e], John Dunbar[e], Dániel G. Knapp[f], Gábor M. Kovács[f], and Andrea Porras-Alfaro[a,g]

[a]Department of Biological Sciences and Institute for Environmental Studies, Western Illinois University, Macomb, Illinois 61455; [b]Department of Biology, University of New Mexico, Albuquerque, New Mexico 87131; [c]Division of Biology, Kansas State University, Manhattan, Kansas 66506; [d]Office of the Provost and Executive Vice President for Academic Affairs, Cedar Falls, Iowa 50614; [e]Los Alamos National Laboratory, Los Alamos, New Mexico 87545; [f]Department of Plant Anatomy, Institute of Biology, Eötvös Loránd University, Budapest, Hungary; [g]Division of Environmental Biology, National Science Foundation, Alexandria, Virginia 22314

ABSTRACT

Darksidea is a common genus of dark septate fungi—a group of ascomycetes in semiarid regions. A survey reported *D. alpha* and a distinct *Darksidea* lineage as abundant root-associated fungi of foundational grasses in North America. Fungi were isolated, and metabarcode data were obtained from sequencing of fungal communities of grass roots in the United States. During a comprehensive investigation of the *Darksidea* lineage, we carried out polyphasic taxonomy, genomic characterization, and identification of host associations, geographic distribution, and environmental factors that correlate with its abundance. For molecular phylogenetic studies, seven loci were sequenced. Isolates of the distinct *Darksidea* had variable colony morphology. No sexual reproductive structures were detected, but chlamydospores were frequently observed. The complete genome of an isolate of the lineage was sequenced with a size of 52.3 Mb including 14 707 gene models. Based on morphology and phylogenetic analysis, we propose the novel species *Darksidea phi*, sp. nov. Metabarcoding data showed that *D. phi* distribution and relative abundance were not limited to semiarid regions or a specific grass species, suggesting low host specificity among graminoids. This new species, *D. phi*, expands the distribution of the genus in the United States beyond prior reports from arid regions.

ARTICLE HISTORY
Received 20 April 2021
Accepted 19 January 2022

KEYWORDS
Andropogon; *Bouteloua*; dark septate endophytes; fungal biogeography; Illumina sequencing; plant symbionts; *Schizachyrium*; 1 new taxon

INTRODUCTION

Root-colonizing endophytes include dark septate fungi (DSF) that are characterized by septate hyphae and dark-pigmented cell walls due to melanin aggregation, which is why they are also commonly called dark septate endophytes (DSEs) (Jumpponen and Trappe 1998; Porras-Alfaro and Bayman 2011). It has been proposed that melanin allows DSF to resist drought, heat, and radiation in desert and alpine ecosystems (Haselwandter and Read 1982; Knapp et al. 2012; Porras-Alfaro et al. 2011; Redman et al. 2002); nevertheless, DSF melanin production had no correlation with trace element and salt stress tolerance as recently shown (Berthelot et al. 2020; Gaber et al. 2020). Dark septate fungi root colonizers are relatively frequent in arid and semiarid grasslands worldwide (Mandyam and Jumpponen 2005), where they inhabit healthy roots of different grass species (Knapp et al. 2019, 2012; Porras-Alfaro et al. 2008).

The order Pleosporales is one of the most common orders in grassland ecosystems, comprising a plethora of grass root endophytes (Jumpponen et al. 2017; Zhang et al. 2012). Several DSF are classified in this order, including various genera such as *Rhizopycnis*, *Periconia*, and *Darksidea*, which are common in semiarid and temperate regions (Knapp et al. 2012; Mandyam et al. 2010; Porras-Alfaro et al. 2008). Description of pleosporalean fungi is typically based on characterization of asci, ascospores, and ascomata; however, many DSF do not produce sexual structures (but see Knapp et al. 2015; Pintye and Knapp 2021), and this characterization has led to inaccurate family designations within the order (Zhang et al. 2012).

The genus *Darksidea* was described by Knapp et al. (2015) to include six congeneric *Darksidea* species: *D. alpha, D. beta, D. delta, D. epsilon, D. gamma*, and *D. zeta*. Members of this genus were isolated from the grass species *Festuca vaginata* and *Stipa borysenthica*. Colony morphology of *D. alpha* is highly variable, and the formation of ascomata with asci and ascospores can be induced in four of the six species (*D. alpha, D. beta,*

CONTACT Andrea Porras-Alfaro aporrasa@nsf.gov
Supplemental data for this article can be accessed on the publisher's Web site.

Published online 08 Apr 2022

D. gamma, and *D. zeta*; Knapp et al. 2015). *Darksidea* represents one of the most common lineages of DSF on semiarid grasses. It was the most abundant DSF on *Bouteloua gracilis* roots (semiarid grass) and in biological soil crusts in central New Mexico (Herrera et al. 2010; Khidir et al. 2010; Porras-Alfaro et al. 2011, 2008). *Darksidea* was also the third most common DSF on grasses of the Great Hungarian Plain in Europe (Knapp et al. 2012). Furthermore, this genus has been reported in Spain, in arid areas of China, and in grasses from Nepal and South Africa (Bokati et al. 2016; Li et al. 2018; Pereira et al. 2019) and represented more than one fourth of root endophytes isolated from the dominant grass *Stipa krylovii* in the Mongolian steppe (Knapp et al. 2019). Because of the transcontinental dominance and abundance of *Darksidea*, the lineage may constitute a key member of the core mycobiome for grasses in arid and semiarid regions across the globe (Knapp et al. 2019, 2012; Porras-Alfaro et al. 2011, 2008).

The *Darksidea* genus harbors a diverse set of species whose functions remain relatively unknown. Rudgers et al. (2022) recently examined the biogeography of fungal root communities of foundational grasses, in which both *Darksidea alpha* and a new *Darksidea* species were abundant among the isolates cultured from roots and detected using Illumina sequencing.

The main objective of this study was the comprehensive characterization of a novel *Darksidea* species from grasses of the central plains in the United States. Our aims were to carry out polyphasic taxonomy, genomic characterization, and identification of the specific host associations, geographic distribution, and environmental factors that correlate with the relative abundance of *Darksidea phi*, sp. nov., proposed here.

MATERIALS AND METHODS

Sample collection and processing.—Cultures of *Darksidea* lineages were isolated from root samples collected in the summer of 2015 as part of a larger project to evaluate the impact of drought, geography, plant traits, and edaphic and environmental factors on fungal communities of grass species across replicated latitudinal gradients in North America. Collection permits and detailed site descriptions were listed in previous publications (Lagueux et al. 2020; Rudgers et al. 2022). Roots of blue grama (*Bouteloua gracilis*), black grama (*B. eriopoda*), buffalo grass (*B. dactyloides*), big bluestem (*Andropogon gerardii*), and little bluestem (*Schizachyrium scoparium*) were collected from 24 sites in west-central plains in the United States. Roots were shipped overnight to Western Illinois University (Macomb, Illinois) and processed within 48 h of collection. The isolates described in this study occurred in 6 of the 24 sites (TABLE 1).

Fungal isolation.—Briefly, 1-cm root segments were surface-sterilized with 70% ethanol for 1 min, followed by 1% sodium hypochlorite for 1 min and then three rinses with distilled autoclaved water. Root areas damaged due to sterilization were removed, and root fragments (2–3 mm) were placed in malt extract agar (MEA) (Difco Laboratories, Sparks, Maryland) amended with antibiotics (streptomycin and tetracycline, 50 mg/L) and incubated at room temperature for 2 wk. Colonies with different morphologies were isolated to establish pure cultures in MEA with antibiotics. Rectangles (1 cm × 4 cm) of actively growing fungi were stored in sterile water at room temperature. Over 1000 fungal isolates were recovered. The holotype specimen of the novel taxon was dried, and, in the form of a biologically inert agar culture, it was deposited in the herbarium of the Hungarian Natural History Museum, Budapest (BP), under the accession number 111489BP (barcode HNHM-MYC-009906). Representative cultures of the novel taxon were deposited at the Centraalbureau voor Schimmelcultures–Westerdijk Fungal Biodiversity Institute (CBS-KNAW) collection under CBS collection numbers CBS 148427–148431. Additional copies of the cultures were also deposited at the University of New Mexico Fungarium (Rudgers, New Mexico), Western Illinois University Fungarium (Macomb, Illinois), the Institute of Biology, Eötvös Loránd University, (Budapest, Hungary), and Los Alamos National Laboratory (Los Alamos, New Mexico).

DNA extraction, amplification, sequencing, and phylogenetic analyses.—Genomic DNA was extracted from pure culture mycelia using a Wizard Genomic DNA

Table 1. Collection sites and plant hosts yielding *Darksidea phi* isolates.

Site	Code	Region	Latitude (°)	Longitude (°)	Plant species
Montevista, Colorado	BLM	West	37.627547	−106.253289	BOGR
Carson National Forest	CNF	West	36.23189	−106.37604	BOER, BOGR
Deming, New Mexico	FMT	West	32.16806	−107.75105	BOGR
Ladybird Johnson Wildlife Center	CAD	Mid	33.307867	−97.6054167	BUDA
Ian Nicholson Audubon	LAR	Mid	40.66462	−98.9063	SCSC
Konza Prairie	KNZ	East	39.0745	−96.6036	BOGR, BUDA, SCSC

Note. BOGR = *Bouteloua gracilis*; BOER = *B. eriopoda*; BUDA = *B. dactyloides*; SCSC = *Schizachyrium scoparium*.

Purification Kit (Promega, Madison, Wisconsin). The nuc rDNA ITS1-5.8S-ITS2 (internal transcribed spacer, ITS) was amplified with polymerase chain reaction (PCR) and sequenced (TABLES 2, 3). Isolates were clustered into operational taxonomic units (OTUs) based on the 97% similarity. Out of the 1033 isolates in the collection, 77 isolates were classified as members of the *Darksidea* genus using the Ribosomal Database Project (RDP) classifier (Cole et al. 2014). Of the 77 isolates, 22 isolates were selected for the sequencing of additional loci to identify lineage placement. For additional phylogenetic analysis, the partial 28S nuc rDNA (large subunit, 28S), partial 18S nuc rDNA (small subunit, 18S), and partial actin (*ACT*), β-tubulin (*TUB*), calmodulin (*CAL*), and translation elongation factor 1-α (*TEF*) were amplified following recommended loci in Knapp et al. (2015) (TABLE 2). Extracted DNA was PCR-amplified with 1 µL of forward and reverse primers (5 µM), 3 µL 1% bovine serum albumin (BSA), 6.5 µL of MilliQ H_2O, and 12.5 µL of GoTaq Green Master Mix (Promega) for a 24-µL master mix plus 1 µL DNA. Negative controls used 1 µL of MilliQ H_2O instead of DNA. The PCR conditions used for ITS, 28S, and 18S; *ACT, CAL*, and *TUB*; and *TEF* are detailed in TABLE 3.

Amplification success was confirmed using gel electrophoresis (1.2% agarose in Tris-acetate-EDTA buffer), and amplicons were sequenced with the respective forward and reverse primers at GENEWIZ (South Plainfield, New Jersey). Resulting sequences were assembled, cleaned, and trimmed using Sequencher 4.1 (Gene Code, Ann Arbor, Michigan).

We combined and aligned sequences of the isolates presented here with those of representative strains of *Darksidea* species using the online version of MAFFT 7 (Katoh et al. 2017) and the E-INS-i method. The alignments were examined and edited in MEGA7 (Kumar et al. 2016). In the phylogeny, *Lentithecium fluviatile* (CBS 122367) and *L. clioninum* (CBS 139694), the closest relatives of the *Darksidea* (see Dayarathne et al. 2018; Haridas et al. 2020; Tanaka et al. 2015; Xu et al. 2020) species, served as outgroups. In this data set, ITS, 28S, 18S, *TEF, TUB, ACT*, and *CAL* sequences were used. Indels were coded from the ITS and 18S regions (Nagy et al. 2012) by the simple indel coding algorithm (Simmons et al. 2001; Young and Healy 2003) with the program FastGap (Borchsenius 2009) and implemented in the alignment as additional two partitions. Therefore, in the multilocus phylogeny, nine partitions were used, and the combined data set consisted of 34 taxa and 5442 characters.

Bayesian inference (BI) analyses were performed with MrBayes 3.1.2 (Ronquist and Huelsenbeck 2003; Ronquist et al. 2012) using a GTR+G substitution model for the nucleotide partitions and the two-parameter Markov (Mk2 Lewis) model for the indel partitions. Four Markov chains were run for 10 million generations sampling every 1000 generations, with a burn-in value set at 4000 sampled trees. A good topological convergence was observed during the Bayesian analysis when the average standard deviation of split frequencies of runs was less than 0.01 and the potential scale reduction factor converged to 1.0. Maximum likelihood (ML) phylogenetic analysis was carried out with the raxmlGUI 1.3 implementation (Silvestro and Michalak 2012; Stamatakis 2014). A GTR+G nucleotide substitution model was used for nucleotide partitions with ML estimation of

Table 2. Loci and forward and reverse primers used for the phylogenetic analysis of *Darksidea phi*.

Locus	Symbol	Forward primer	Reverse primer
nuc rDNA ITS1-5.8S-ITS2	ITS	ITS1F (Gardes and Bruns 1993)	ITS4 (White et al. 1990)
partial 28S nuc rDNA	28S	LR0R (Schoch et al. 2012)	LR5 (Schoch et al. 2012)
partial 18S nuc rDNA	18S	NS1 (White et al. 1990)	NS4 (White et al. 1990)
partial actin	*ACT*	ACT-512 F (Carbone and Kohn 1999)	ACT-2Rd (Quaedvlieg et al. 2011)
partial calmodulin	*CAL*	CAL-228 F (Carbone and Kohn 1999)	CAL-2Rd (Groenewald et al. 2013)
partial β-tubulin	*TUB*	CYLTUB1F (Groenewald et al. 2013)	Bt-2b (Glass and Donaldson 1995)
partial translation elongation factor 1-α	*TEF*	EF1-728 F (Carbone and Kohn 1999)	EF-2Rd (Groenewald et al. 2013)

Table 3. Loci and PCR conditions used for the phylogenetic characterization of *Darksidea phi*.

Locus	Initial denaturation	35 cycles	Final elongation
nuc rDNA ITS1-5.8S-ITS2 partial 28S nuc rDNA partial 18S nuc rDNA	95 C, 5 min	Denaturation: 94 C, 30s Annealing: 50 C, 30s Elongation: 72 C, 45s	72C, 7 min
partial actin partial calmodulin partial β-tubulin	95 C, 5 min	Denaturation: 95 C, 30s Annealing: 55 C, 30s Elongation: 72 C, 40s	72C, 5 min
partial translation elongation factor 1-α	95 C, 5 min	Denaturation: 94 C, 30s Annealing: 64.9 C, 30s Elongation: 72 C, 40s	72C, 5 min

base frequencies, and the indel data were treated as binary data. ML bootstrap (BS) analysis with 1000 replicates was used to test the support of the branches. Phylogenetic trees were visualized and edited in MEGA7 (Kumar et al. 2016) and deposited in TreeBASE (www.treebase.org) as study 26 440.

Genome sequencing.—Isolate DS919, the type culture of the distinct *Darksidea* lineage, was grown on MEA, and the MP FastDNA Spin Kit for Soil DNA was used to extract DNA (MP Biomedicals, Irvine, California). Three plugs were transferred into bead-beater tubes containing sodium phosphate buffer and MT lysis buffer and frozen overnight at −80 C prior to extraction per the manufacturer's recommendations. Extraction products were visualized with gel electrophoresis to confirm size and quality.

Illumina NextSeq 550 libraries were prepared as previously described (Albright et al. 2018) and sequenced using the NextSeq Mid-Output Kit to produce 150-bp paired-end reads (illumina, Inc, San Diego, California). Libraries were diluted, pooled, and denatured before 300 cycles of sequencing. Prior to assembly, reads were curated to remove adapters and PhiX sequence contamination using the BBDuk command in the BBTOOLS package (Bushnell et al. 2017). Curating parameters included a hamming distance of 2, a minimum Q-score of 10, and a minimum k-mer size of 8. Paired-end reads were trimmed to the same length and then assembled with SPAdes 3.13.1 (Bankevich et al. 2012) at default k-mer settings. Assembly quality was evaluated with QUAST 5.0.2 (Gurevich et al. 2013) and FastQC 0.11.8 (Andrews 2010). To assess genome completeness, the lineage data set "pleosporales_odb10" and default settings were set in BUSCO 4.0.5 (Simão et al. 2015). *Aspergillus nidulans* was used as the reference genome to annotate genes in AUGUSTUS 3.3.3 (Stanke et al. 2004). The genome of DS919 was deposited in the Sequence Read Archive as BioProject PRJNA637112.

Culture morphology.—Out of five isolates we used three representative isolates of the distinct *Darksidea* group (DS919, DS925, DS697) for morphological characterization. These isolates represented colony morphology and color variation for the isolates in this group. Inoculum was initially grown on MEA with chloramphenicol (0.5 g/L) (Research Products International, Mt. Prospect, Illinois). To stimulate sexual and asexual sporogenesis, we excised 5-mm-diam plugs from 2-wk-old cultures and then plated them onto one of 13 different media (SUPPLEMENTARY TABLE 1), including MEA, water agar (WA), Emerson agar (EA), synthetic nutrient poor agar (SNA), dichloranglycerol agar (DG18), Leonian agar (LA), Czapek-Dox agar (CDA), potato dextrose agar (PDA), soil agar (SA), modified Melin-Norkrans (MMN), kiwicha agar (100 g/L of kiwicha flour and 15 g/L of agar) with chloramphenicol (0.5 g/L) (KIWI), quinoa agar (100 g/L of quinoa flour and 15 g/L of agar) with chloramphenicol (0.5 g/L) (QUI), or oatmeal agar (100 g/L of oatmeal flour and 15 g/L of agar) with chloramphenicol (0.5 g/L) (OAT) (SUPPLEMENTARY TABLE 1). Cultures were incubated for 20 d at room temperature (25 C) and a 6210 RAL Chart K7-2014 (Elcometer, Warren, Michigan) was used to describe standard colors of the colonies. Other methods were tested to promote sporogenesis, including the use of different plant materials, as described in Knapp et al. (2015), but they did not provide positive results and are not further discussed in this article.

Microscopy.—Two-week-old cultures with potential reproductive structures were used to prepare slide cultures. For slide cultures, we inoculated fungi on 1 cm × 1 cm medium squares placed on glass Petri dishes (Riddell 1950). One wet sterile cotton ball was added per Petri dish to keep the cultures moist. Slide cultures were incubated at room temperature for 2 wk. We prepared the slide cultures for microscopic observation by placing the cover slide over drops of a solution of lactophenol cotton blue:water (1:2) and observing any microscopic structures using a phase contrast microscope at 200×–400× magnification (Leica Microsystems DM1000; Buffalo Grove, IL).

Next-generation metabarcoding.—*Darksidea* sequences were extracted from sequence data obtained from 24 sites and five grass species as reported in Lagueux et al. (2020), Rudgers et al. (2021), and Rudgers et al. (2022). Briefly, DNA from roots of *B. gracilis, B. eriopoda, B. dactyloides, S. scoparium*, and *A. gerardii* collected from the 24 sites was extracted with MoBio Power Soil DNA Isolation Kit (MoBio, Carlsbad, California). The ITS2 region of the ribosomal RNA was amplified with primers fITS7 (Ihrmark et al. 2012) and ITS4 (White et al. 1990). Quality-controlled and screened sequences were clustered into OTUs at a 97% sequence similarity threshold, and abundance data were rarefied to 10 000 reads per sample. Sequence data of the distinct *Darksidea* lineage were extracted to use in the analysis of host specificity and distribution.

To examine the geographic distribution and host associations of the novel *Darksidea* lineage, we fitted linear

mixed-effects models that predicted relative abundance from latitude. Models included the main effects of plant species, latitude, and their interaction as fixed effects, and collection site and replicated longitudinal gradient (west, central, east; TABLE 1) as random effects. The total number of Illumina-based sequences of the distinct lineage was natural log–transformed (ln(X + 1) to spread the variance of the data and meet the assumption of homogeneity of variances and normality of residuals. The analysis was repeated for geographic traits (longitude and elevation), plant traits (specific leaf area), and edaphic (ammonium, nitrate, phosphorus, pH, and soil organic matter) and climate (soil gravimetric water content, growing degree days [GDDs] for 2015, GDDs of 3 years, GDDs of 30 years, annual precipitation of 2015, average annual precipitation of 3 years, and average annual precipitation of 30 years) factors in place of latitude in order to explore geographic, abiotic, and plant trait correlates of the distinct *Darksidea* lineage relative abundance. These environmental correlate models were ranked by their relative importance in explaining lineage relative abundance using model selection procedures with the second-order small sample–corrected Akaike information criterion (AICc) (package MuMln 1.43.6) (Barton 2019). All statistical analyses were done with the lmer function in LME4 package 1.1-21 (Bates et al. 2015). Heat maps were constructed using GGPLOT2 3.2.1 (Wickham 2016) and GGMAP 3.0.0 (Kahle and Wickham 2013).

RESULTS

Phylogenetic analysis.—Based on multilocus phylogeny (FIG. 1) of the 22 isolates representing *Darksidea* species selected from those obtained from grasses in our latitudinal survey, 11 isolates clustered with *D. alpha*, one isolate (DS1424) belonged to *D. zeta*, and another (DS1406) represented a distinct lineage in sister position with *D. epsilon* and *D. delta*. We identified no isolates representative of *D. delta, D. epsilon, D. gamma*, or *D. beta* in our culture collection. Four isolates (DS241 and DS246; DS318 and DS926) represented two clades close to *D. alpha*. Additionally, five isolates (DS193, DS194, DS211, DS919, DS1626) clustered together and represented a well-supported (ML bootstrap [BS] = 100, posterior probability [PP] = 1) clade different from *D. gamma* and *D. beta* that we propose as a novel taxon—*D. phi*, sp. nov.

Genome sequencing.—NextSeq sequencing resulted in approximately 40.37 million reads, of which 40.35 million passed quality control. After assembly, 979 scaffolds greater than or equal to 500 bp were produced, with an overall N_{50} of 160 354 bp and a total length of 52.3 Mb. The assembled genome of DS919 showed a marked compartmentalization of contigs, with a low GC peak of approximately 21%, a high GC peak of approximately 51%, and an overall GC content of 47% (Submission ID: SUB7459143, BioProject ID: PRJNA637112). The genome of DS919 was estimated to be 91.9% complete according to BUSCO, with 6076 single-copy BUSCOs, 24 complete and duplicated BUSCOs, 55 fragmented BUSCOs, and 486 missing BUSCOs out of a total 6641 that were searched. AUGUSTUS predicted 14 707 protein-coding genes.

Biogeography.—*Darksidea phi* sequences were present in all 24 sites surveyed using Illumina sequencing (only recovered in culture from six sites). In general, *D. phi* had low host specificity and wide geographic distribution (FIGS. 4 and 5). Latitude was a significant predictor ($P < 0.05$) of *D. phi* relative sequence abundance among sites and host plant species, and a better predictor than longitude (ΔAICc = 10.28). Elevation was not a significant predictor ($P > 0.05$) of *D. phi* relative abundance; however, it is a better predictor than longitude (ΔAICc = 14.18). The largest relative abundances of *D. phi* sequences occurred in southwestern sites, particularly New Mexico (1666 sequences, rarefied data) and west Texas (BNP, DMT, and GMT, 464 sequences) (FIG. 4, SUPPLEMENTARY TABLE 2). *Darksidea phi* relative abundance was intermediate at central sites in Texas (CAD and LBJ, 304 sequences), southeast Texas (SFA, 289 sequences), and Oklahoma (FCP and KAE, 301 sequences). Northeast and eastern sites within our survey region had the lowest relative abundances (SCP, NWP, KNZ, ONF, and UHC, 99 sequences).

Host association.—Host species identity was the most important factor determining abundance of *D. phi* sequences over our sampling region in south central states in the United States ($P < 0.0001$). *Darksidea phi* was more abundant in *B. gracilis* and *B. eriopoda* than in the other grasses sampled. Specifically, *Bouteloua gracilis* (2142 sequences) and *B. eriopoda* (1027 sequences) had a greater relative abundance of sequences than *S. scoparium* (560 sequences), *B. dactyloides* (330 sequences), or *A. gerardii* (69 sequences) (FIG. 5). Within a grass species, westernmost sites had the greatest abundance and number of sequences detected compared with easternmost sites (longitude, $P > 0.05$; longitude × host species, $P = 0.45$), but this was not independent

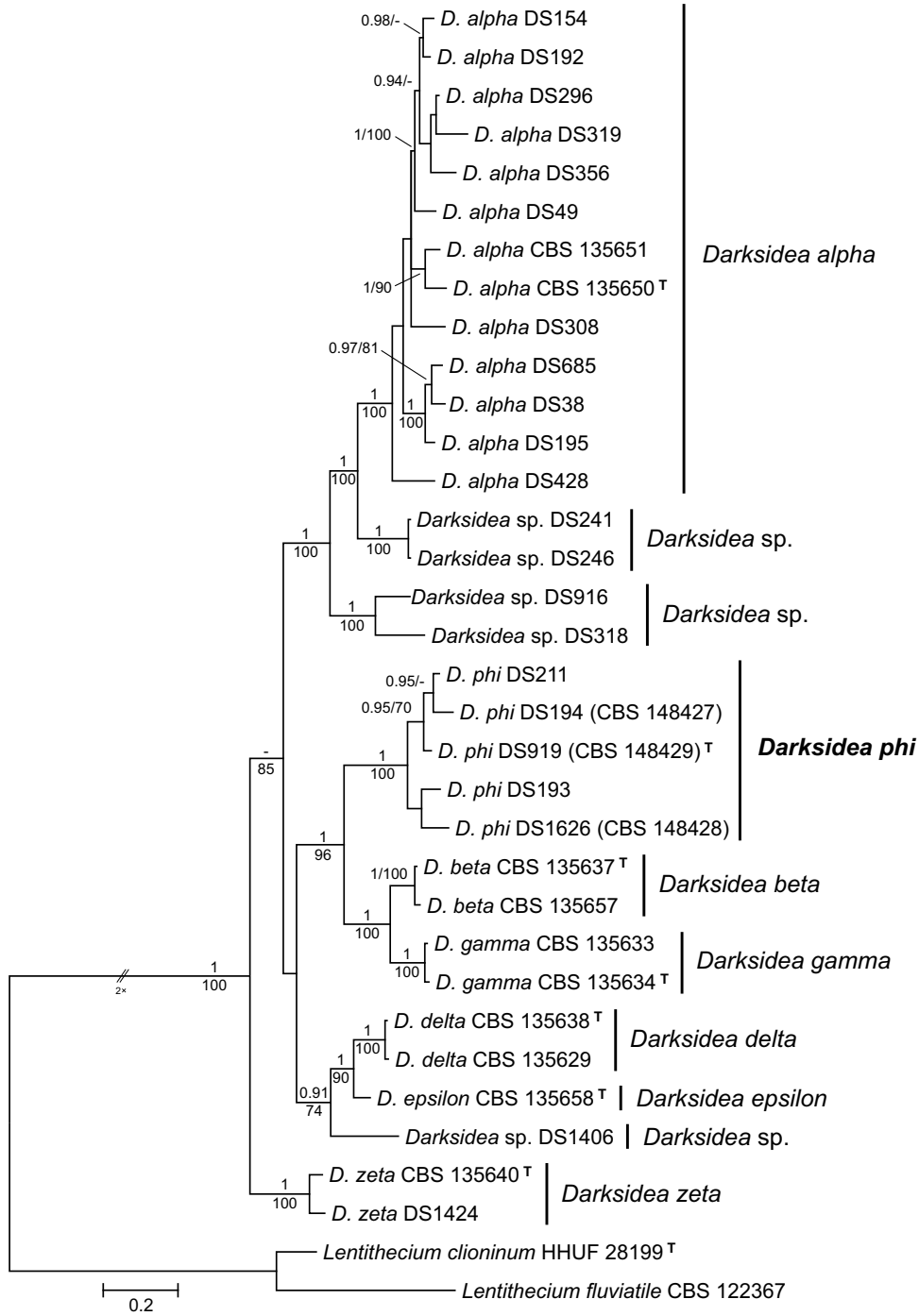

Figure 1. Phylogenetic tree of *Darksidea phi* and representatives of other *Darksidea* species. Strains presented in this study are coded with the letters DS. The 50% majority rule consensus phylogram inferred from the Bayesian analysis of the combined data set of seven loci (ITS, 28S, 18S, TEF, TUB, ACT, CAL) and coded indels from ITS and 18S as two additional partitions. Bayesian posterior probabilities (≥0.90) are shown before slashes or above branches; ML bootstrap support values (≥70) are shown after slashes or below branches. *Lentithecium fluviatile* (CBS 122367) and *L. clioninum* (CBS 139694) served as multiple outgroups. The bar indicates 0.2 expected changes per site per branch.

of the fact that *B. eriopoda* occurred only on the westernmost latitudinal gradient. Furthermore, host plant species interacted with latitude to influence the relative abundance of *D. phi* sequences (FIG. 6). *D. phi* sequences slightly increased poleward in *B. eriopoda*. However, *D. phi* relative abundance declined poleward on *B. gracilis, B. dactyloides, A. gerardii*, and *S. scoparium* (FIG. 6).

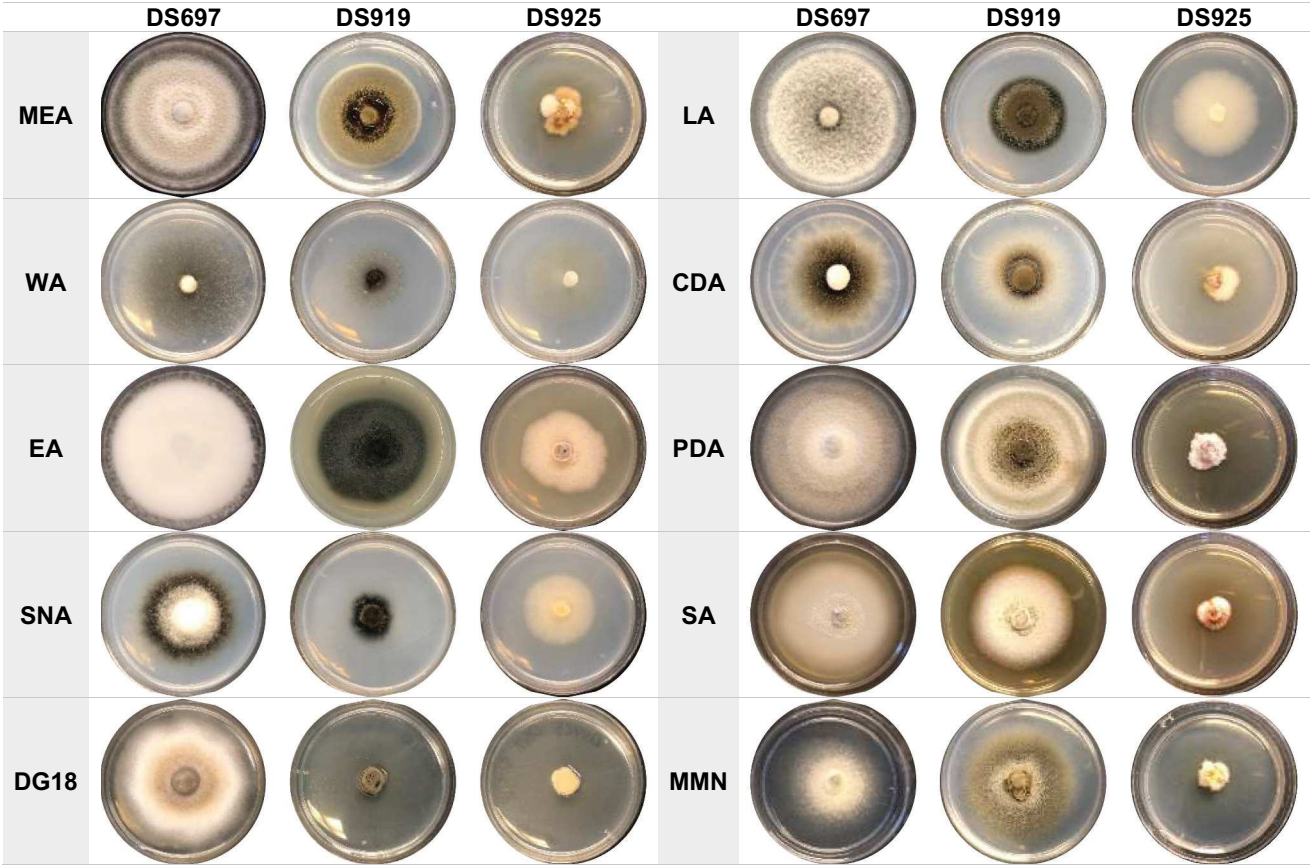

Figure 2. Colonies of three *D. phi* isolates (DS697, DS919, and DS925) in 10 different media (MEA, malt extract agar; WA, water agar; EA, Emerson agar; SNA, synthetic nutrient poor agar; DG18, dichloran-glycerol agar base; LA, Leonian agar; CDA, Czapek-Dox agar; PDA, potato dextrose agar; SA, soil agar; MMN, modified Melin-Norkrans) after 20 d at room temperature showing large morphological variation across isolates and medium types.

Environmental correlates.—We ranked the relative importance of geographic, climatic, edaphic, and plant trait factors as correlates of the rarefied relative abundance of *D. phi*. The best model based on the AICc for model selection was growing degree days (3 years), which explained 12% of variation in relative abundance (marginal R^2 = 0.12). The following factors predicted *D. phi* relative abundance in decreasing order of importance: elevation (16%), latitude (12%), specific leaf area (SLA; 7%), phosphorus (9%), and ammonium (10%). Models including soil gravimetric water content, average soil moisture, pH, and precipitation explained the least variation in abundance of *D. phi* using AICc, and these predictors did not have statistically significant relationships with relative abundance.

TAXONOMY

Darksidea phi M.-J. Romero-Jiménez & A. Porras-Alfaro, sp. nov.

MycoBank MB833647

Typification: USA. KANSAS: Geary County, Manhattan, Konza Prairie Biological Station, latitude: 39.074°, longitude: −96.6036°, in the root of *Bouteloua dactyloides*, summer of 2015, holotype BP111489, type culture DS919 = CBS 148429. GenBank: ITS = MK809001; 28S = MT002089; 18S = MT002109; *ACT* = MN967043; *TUB* = MN982922; *CAL* = MT321321; *TEF* = MT321337.

Etymology: Referring to the letter of the Greek alphabet that represents the golden ratio.

Diagnosis: *D. phi* differs from *D. alpha* (DSE7/24 = CBS 135650 type culture) by unique fixed alleles in the ITS, 28S, 18S, *ACT, TUB, CAL*, and *TEF* loci based on alignments of each locus deposited in TreeBASE as study S26440: ITS positions: 33 (C), 36 (T), 40 (T), 63 (G), 64 (A), 89 (T), 108 (deletion), 131 (A), 152 (T), 158 (T), 161 (G), 165 (A), 202 (T), 397 (T), 489 (C), 512 (A); 28S positions: 56 (C), 58 (G), 59 (G), 116 (T), 159 (T), 187 (C), 191 (T), 222 (A), 424 (C), 430 (G), 455 (T), 493 (A), 499 (A), 500 (C), 517 (T); 369 (T), 411 (A); *ACT* positions: 29 (A), 43 (T), 45 (A), 48 (C), 53 (C), 158 (T), 160 (C), 163 (C), 173 (T), 174 (C), 181 (G), 199 (A), 260

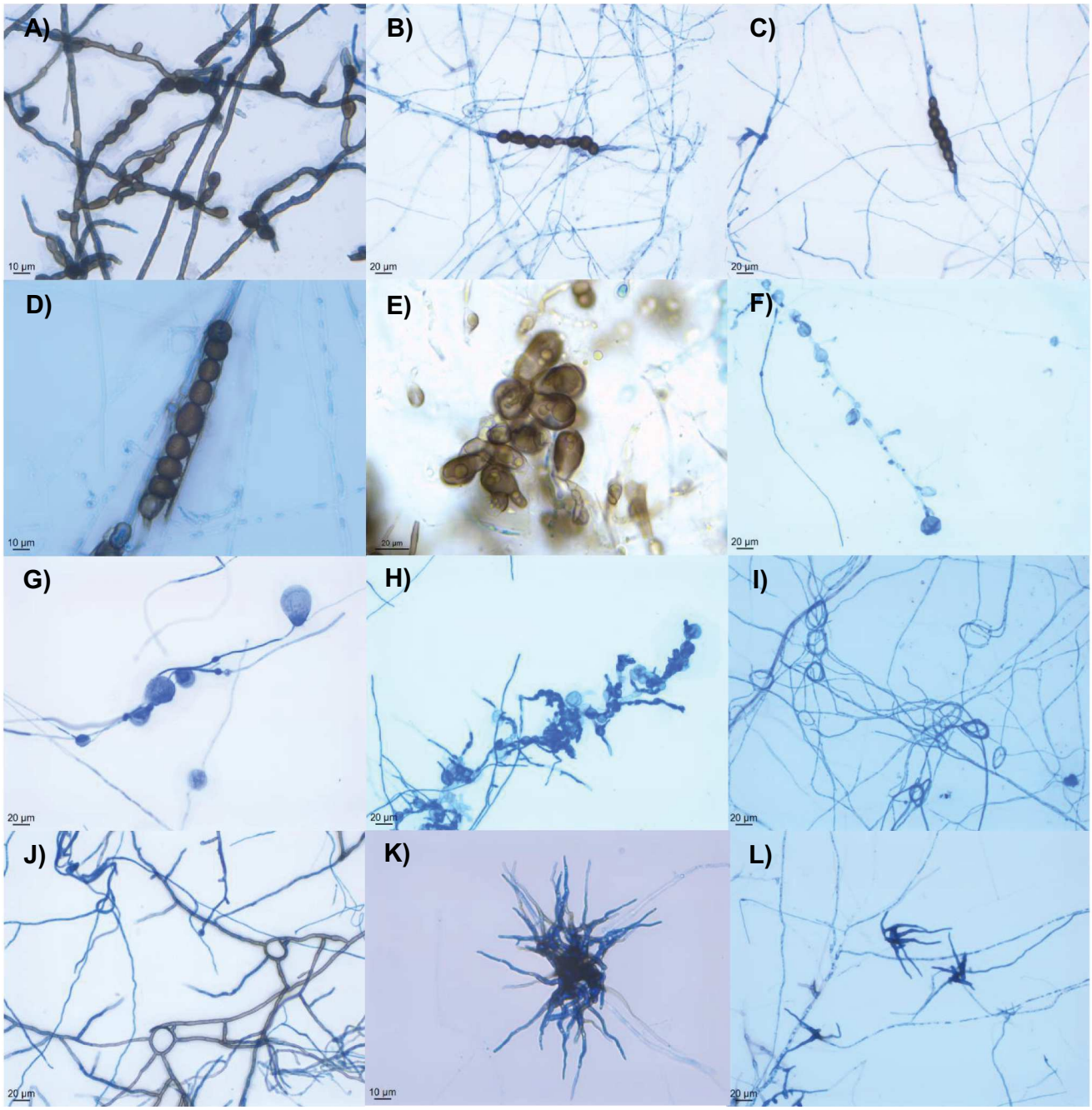

Figure 3. Chlamydospores, vesicle-like structures, hyphal coils, and clustered hyphae produced by *D. phi*. Chlamydospores of DS194 in KIWI (A) and DS697 in QUI (B–D). Vesicle-like structures of DS697 in MEA (E, F), DS697 in KIWI (G), and DS1626 in QUI (H). Hyphal coils of DS1626 in KIWI (I) and DS919 in QUI (J). Clustered hyphae of DS697 in MEA (K) and DS697 in KIWI (L). Bars: A, D, K = 10 µm; B, C, E, F, G, H, I, J, L = 20 µm.

(G), 323 (T), 503 (T); *TUB* positions: 100 (T), 106 (G), 125 (C), 161 (T), 162 (G), 195 (T), 225 (A), 247 (A), 253 (C), 255 (C), 258 (A), 328 (C), 370 (T), 397 (T); *CAL* positions: 9 (C), 25 (A), 29 (G), 33 (G), 35 (C), 39 (C), 110 (T), 118 (A), 120 (G), 128 (A), 153 (C), 160 (T), 161 (T), 181 (T), 184 (A), 196 (C), 246 (G), 272 (A), 297 (G), 336 (C), 429 (G), 464 (C), 509 (A), 516 (C), 521 (A), 524 (A), 527 (C); *TEF* positions: 45 (G), 113 (G), 114 (A), 123 (T), 137 (A), 154 (T), 184 (G), 193–195 (deletion), 200 (C), 226 (C), 229 (T), 236 (T), 239 (T), 407 (C), 410 (C), 420 (C), 437 (G), 441 (A), 465 (C), 501 (T), 576 (T), 645 (C), 661 (A), 729 (C), 765 (T), 876 (T), 880 (T), 881 (C), 976 (T).

Type culture: Darksidea phi, sp. nov., presented a variety of morphologies depending on the medium (FIG. 2). The type culture DS919 had raised mycelium with smooth margins in DG18, EA, and PDA but produced flat mycelium with smooth margins in LA,

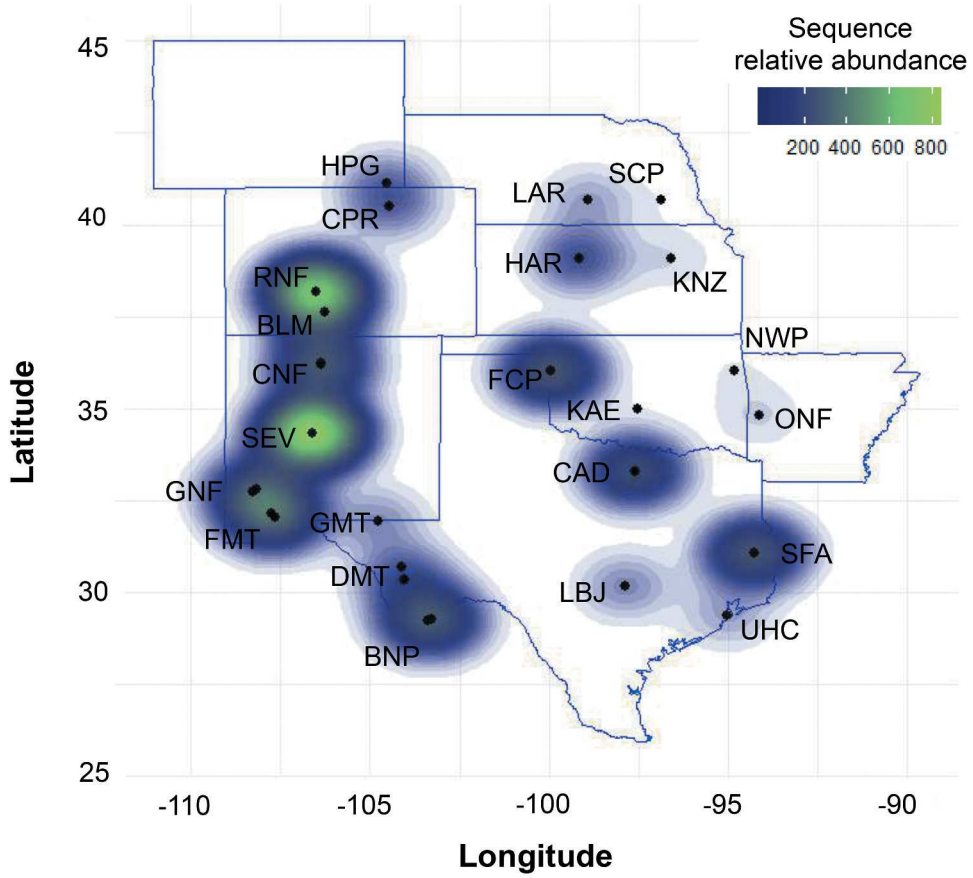

Figure 4. Geographic heat map showing *Darksidea phi* sequence relative abundance and distribution in the Great Plains states of the United States based on Illumina sequencing.

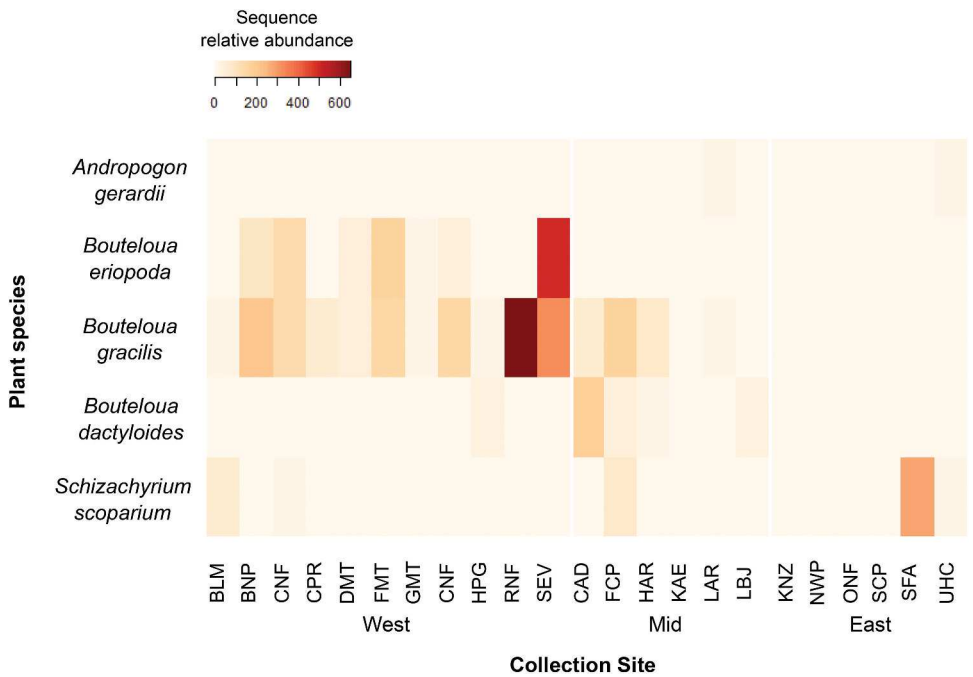

Figure 5. Heat map of *D. phi* Illumina sequence relative abundance and distribution by plant species (*A. gerardii, B. eripoda, B. gracilis, B. dactyloides*, and *S. scoparium*) and region (West, Mid, and East).

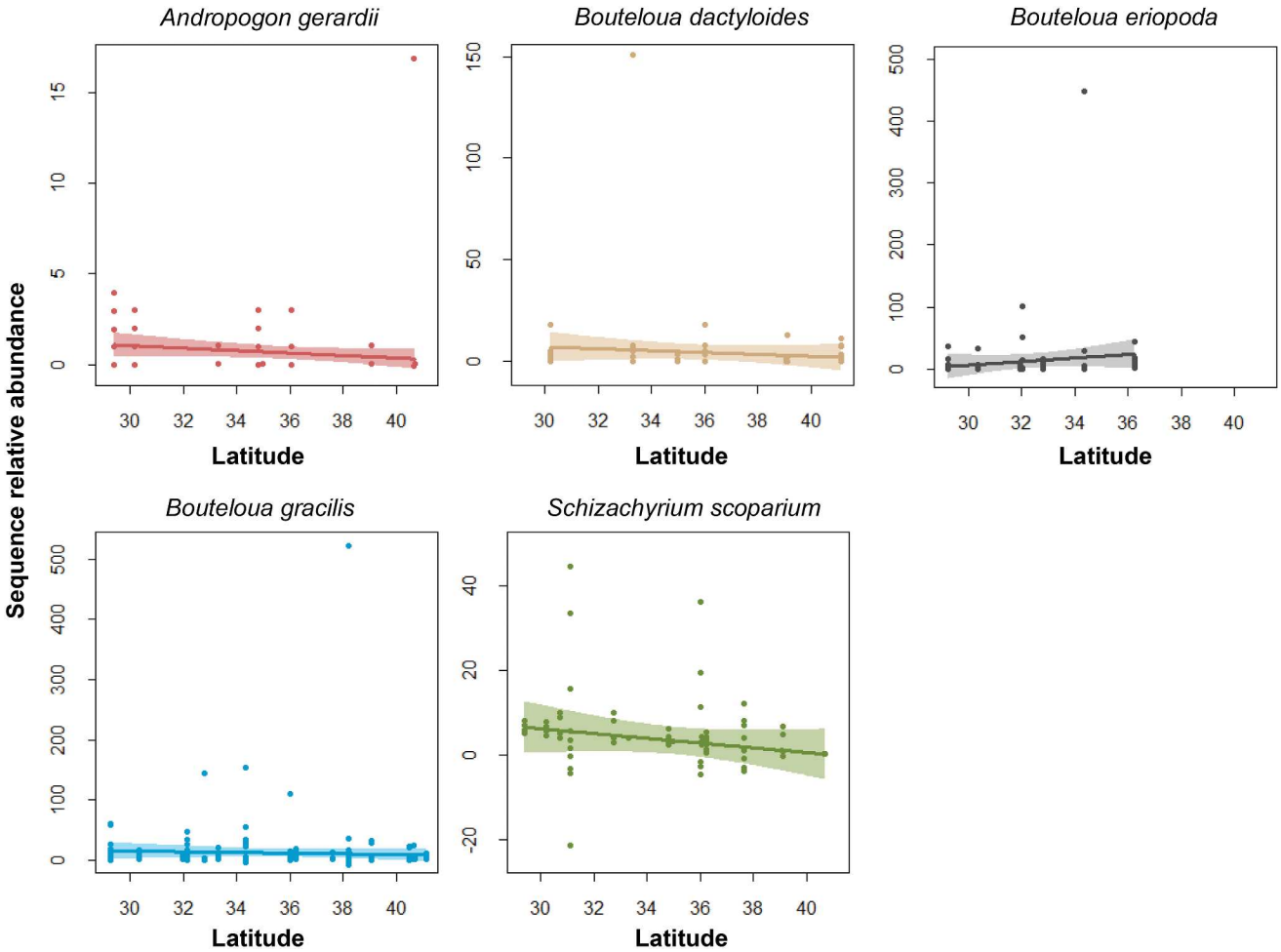

Figure 6. *Darksidea phi* sequence relative abundance by latitude and host plant species (*A. gerardii, B. dactyloides, B. eripoda, B. gracilis*, and *S. scoparium*).

MEA, and SA. Flat mycelium with branched margins was observed in SNA, WA, CDA, and MMN. Mycelium color was quartz gray in DG18, cement gray in EA, green gray and tarpaulin gray in LA, graphite gray and granite gray in SNA, moss gray in WA, ocher yellow and gray beige in MEA, khaki gray, beige and light ivory in PDA, cream and olive brown in CDA, yellow gray in MMN, and light ivory in SA. The colony of DS919 produced exudates (guttate) on DG18, EA, MEA, MMN, and PDA. DS919 formed concentric circles. Colony diameter of DS919 after 4 d at room temperature was 14.5 mm in MEA, 19.2 mm in PDA, 7.7 mm in CDA, 14.5 mm in MMN, and 12.0 mm in SA. After 20 d at room temperature the colony diameter of DS919 was 8.2 mm in DG18, 43.2 mm in EA, 26.6 mm in LA, 15.5 mm in SNA, and 19.4 mm in WA. Hyphae produced by DS919 were hyaline or melanized when cultured in MEA, KIWI, OAT, and QUI. In these media, septate hyphae developed by DS919 were curvy, clustered, branched, and straight. DS919 also formed hyphal coils, chlamydospores, oils, and vesicle-like structures (FIG. 3).

Host: *Darksidea phi* colonized roots of *Bouteloua gracilis, B. eripoda, B. dactyloides, Andropogon gerardii*, and *Schizachyrium scoparium*. These plants belong to the Poaceae family and require low to medium water to survive. In general, they grow on prairies and plains. *Bouteloua gracilis* is a short turf grass highly abundant in the Great Plains of the United States that has high tolerance to cold, heat, and drought (Lady Bird Johnson Wildflower Center 2012). Among the five grass species, where *D. phi* was isolated, *B. gracilis* has the highest drought tolerance. *Bouteloua eriopoda* is a turfgrass not as widely distributed as *B. gracilis*. It grows as a mixed prairie with *B. gracilis, B. dactyloides*, and *B. curtipendula* (Lady Bird Johnson Wildflower Center 2009). *Bouteloua dactyloides* is also a turf grass dominant in shortgrass prairies. It is less drought tolerant than *B. gracilis* (Lady Bird Johnson Wildflower Center 2018). *Andropogon gerardii* is a native

Table 4. Fungal species, isolate numbers, host plants, collection sites, and GenBank accession numbers (ITS, 28S, 18S, *ACT, TUB, CAL*, and *TEF*) of all the fungal isolates used.

				GenBank accession numbers[b]						
Species	Isolate number	Host plant	Collection site[a]	ITS	28S	18S	*ACT*	*TUB*	*CAL*	*TEF*
Lentithecium fluviatile	CBS 122367	*Populus* sp.	Mt. Delpont, France	—	GU301825	GU296158	scaffold_5: 699410–700032	scaffold_8: 319488–319865	scaffold_9: 977832–978438	GU349074
L. clioninum	CBS 139694 ^{T}	—	Hokkaido, Japan	LC014566	AB807540	AB797250	—	—	—	AB808515
Darksidea alpha	CBS 135650 ^{T}	*Festuca vaginata*	Fülöpháza, Hungary	KP183998	KP184019	KP184049	KP184102	KP184214	KP184131	KP184166
	CBS 135651	*F. vaginata*	Fülöpháza, Hungary	KP183996	KP184017	KP184064	KP184087	KP184215	KP184132	KP184167
	DS38	*Andropogon gerardii*	LBJ National Grasslands	MK808738	MT002071	MT002093	MN967027	MN982905	MT321304	MT321323
	DS49	*Bouteloua dactyloides*	LBJ National Grasslands	MK808785	MT002072	MT002094	MN967028	MN982906	MT321305	MT321324
	DS154	*B. gracilis*	Ladybird Johnson Wildlife Center	MK808429	MT002073	MT002095	MN967029	MN982907	MT321306	MT321325
	DS192	*B. dactyloides*	Ladybird Johnson Wildlife Center	MK808578	MT002074	MT002096	MN967030	MN982908	MT321307	MT321326
	DS195	*B. dactyloides*	Ladybird Johnson Wildlife Center	MK808581	MT002077	MT002099	MN967031	MN982911	MT321310	MT321328
	DS296	*B. gracilis*	Guadalupe Mountains National Park	MK808668	MT002081	MT002102	MN967035	MN982915	MT321314	MT321332
	DS308	*B. gracilis*	Guadalupe Mountains National Park	MK808680	MT002082	MT002103	MN967036	MN982916	MT321315	MT321333
	DS319	*B. eriopoda*	Guadalupe Mountains National Park	MK808689	MT002084	MT002105	MN967038	MN982918	MT321317	MT321334
	DS356	*B. eriopoda*	Guadalupe Mountains National Park	MK808725	MT002085	MT002106	MN967039	MN982919	MT321318	—
	DS428	*B. eriopoda*	Big Bend Natural Park	MK808749	MT002086	—	MN967040	—	MT321319	MT321335
	DS685	*B. gracilis*	Konza Prairie	MK808868	MT002087	MT002107	MN967041	MN982920	MT321320	—
Darksidea sp.	DS241	*B. dactyloides*	Ladybird Johnson Wildlife Center	MK808618	MT002079	—	MN967033	MN982913	MT321312	MT321330
	DS246	*B. dactyloides*	Ladybird Johnson Wildlife Center	MK808623	MT002080	MT002101	MN967034	MN982914	MT321313	MT321331
Darksidea sp.	DS916	*B. dactyloides*	Konza Prairie	MK808998	MT002088	MT002108	MN967042	MN982921	—	MT321336
	DS318	*B. eriopoda*	Guadalupe Mountains National Park	MK808688	MT002083	MT002104	MN967037	MN982917	MT321316	—
D. beta	CBS 135637 ^{T}	*F. vaginata*	Fülöpháza, Hungary	KP183978	KP184023	KP184074	KP184112	KP184201	KP184153	KP184189
	CBS 135657	*F. vaginata*	Fülöpháza, Hungary	KP183977	KP184009	KP184075	KP184113	KP184221	KP184150	KP184190
D. gamma	CBS 135633	*F. vaginata*	Fülöpháza, Hungary	KP183984	KP184031	KP184072	KP184110	KP184198	KP184149	KP184187
	CBS 135634 ^{T}	*F. vaginata*	Fülöpháza, Hungary	KP183985	KP184028	KP184073	KP184111	KP184199	KP184151	KP184188
D. delta	CBS 135629	*F. vaginata*	Fülöpháza, Hungary	KP183980	KP184006	KP184067	KP184106	KP184194	KP184144	KP184183
	CBS 135638 ^{T}	*F. vaginata*	Fülöpháza, Hungary	KP183981	KP184024	KP184069	KP184107	KP184102	KP184145	KP184184
D. epsilon	CBS 135658 ^{T}	*Stipa borysthenica*	Fülöpháza, Hungary	KP183983	KP184029	KP184070	KP184109	KP184222	KP184147	KP184186
D. phi	DS193	*Bouteloua dactyloides*	Ladybird Johnson Wildlife Center	MK808579	MT002075	MT002097	—	MN982909	MT321308	MT321327
	DS194 CBS 148427	*B. dactyloides*	Ladybird Johnson Wildlife Center	MK808580	MT002076	MT002098	—	MN982910	MT321309	—
	DS211	*B. dactyloides*	Ladybird Johnson Wildlife Center	MK808594	MT002078	MT002100	MN967032	MN982912	MT321311	MT321329
	DS697 CBS 148431	*B. gracilis*	Konza Prairie	—	—	—	—	—	—	—
	DS919 ^{T} CBS 148429 ^{T}	*B. dactyloides*	Konza Prairie	MK809001	MT002089	MT002109	MN967043	MN982922	MT321321	MT321337
	DS925 CBS 148430	*Schizachyrium scoparium*	Konza Prairie	—	—	—	—	—	—	—
	DS1626 CBS 148428	*B. gracilis*	Carson National Forest	MK808491	MT002092	MT002111	—	MN982925	—	—
D. zeta	CBS 135640 ^{T}	*F. vaginata*	Fülöpháza, Hungary	KP183979	KP184013	KP184071	KP184115	KP184204	KP184148	KP184191
Darksidea sp.	DS1406	*B. dactyloides*	High Plain Grassland	MK808347	MT002090	—	MN967044	MN982923	—	—

[a]Texas: Ladybird Johnson Wildlife Center; Kansas: Konza Prairie; New Mexico: Carson National Forest.
[b]ITS, nuc rDNA ITS1-5.8S-ITS2; 28S, partial 28S nuc rDNA; 18S, partial 18S nuc rDNA; *ACT*, partial actin; *TUB*, partial β-tubulin; *CAL*, partial calmodulin; *TEF*, partial translation elongation factor 1-α.

bunchgrass distributed in prairies and low meadows across several states in the United States. Its drought tolerance is greater when it grows in deep prairies (Lady Bird Johnson Wildflower Center 2015). *Schizachyrium scoparium* is another native bunchgrass in the United States that requires low quantities of water and is tolerant to drought and different types of soils (Lady Bird Johnson Wildflower Center 2019).

Distribution: *Darksidea phi* occurred in several states of the Great Plains in the United States, including Wyoming, Colorado, New Mexico, Texas, Oklahoma, Kansas, Nebraska, and Arkansas. Latitude of the sites ranged from 29.23° to 41.12° (FIG. 4). *Darksidea phi* was isolated in longitudes from −108.29° to −94.13° where mean annual precipitation is around 1000 mm. *Darksidea phi* was detected on sites where elevations range from −20 to 2747 mts, with an average soil moisture percentage of 1.18% to 33.99%. Soils in the sites had a pH of 5 up to 8, a soil organic matter content from 0.7 to 8.9%, and soil gravimetric water content of 0.01 and 0.51%.

Culture morphology: *Darksidea phi* isolates had clear differences in color, morphology, and production of metabolites depending on the source medium (FIG. 2). *Darksidea phi* isolates spanned a variety of colors, including signal white (RAL 9003), oyster white (RAL 1013), brown beige (RAL 1011), silk gray (RAL 7044), olive gray (RAL 7002), olive brown (RAL 8008), yellow gray (RAL 7034), green gray (RAL 7009), light ivory (RAL 1015), and cream (RAL 9001). Morphology of *D. phi* on PDA and SA did not vary among multiple isolates. However, *D. phi* morphology and growth rate were highly variable among isolates when grown on MEA, Emerson, Leonian, or SNA media. Generally, *D. phi* isolates grew faster on PDA, MEA, or Emerson than on SNA, DG18, or WA. *Darksidea phi* mycelium ranged from smooth (DS919 in MEA) to branched (DS697 in CDA) edges, flat (DS925 in Emerson) to aerial (DS697 in EA) morphology, and with nonconcentric (DS697 in EA) or concentric (DS697 in MEA and DS919 in PDA) rings. Multiple *D. phi* isolates produced guttation droplets on select media; isolate DS925 on DG18, PDA, MMN, and EA; DS697 on PDA; and DS919 on DG18, EA, MEA, MMN, and PDA.

Microscopy: *Darksidea phi* produced a wide variety of microscopic structures depending on the medium used for culture (FIG. 3). Several isolates produced chlamydospores connected through melanized hyphae (FIG. 3A) and hyaline hyphae (FIG. 3B–D). Vesicle-like structures with (FIG. 3E) and without (FIG. 3F–H) oils, hyaline (FIG. 3I) and pigmented (FIG. 3J) hyphal coils, and clustered hyphae (FIG. 3K–L) were observed in several isolates of *D. phi*. *Darksidea phi* also had diverse hyphal architecture (SUPPLEMENTARY FIG. 1). Septa were observed in both hyaline (SUPPLEMENTARY FIG. 1a) and melanized (SUPPLEMENTARY FIG. 1b) hyphae. Highly branched (SUPPLEMENTARY FIG. 1c–e) and curly (SUPPLEMENTARY FIG. 1f–h) hyphae were also observed in several isolates. Clear differences in hyphal pigmentation were observed among different *D. phi* isolates (SUPPLEMENTARY FIG. 1i–l).

Notes: Darksidea phi isolates are morphologically diverse and produce a variety of microscopic structures that are shared with *D. alpha*. Unlike *D. alpha, D. zeta*, and *D. beta*, cultures of *D. phi* have not produced sexual structures. In the roots of foundational grasses at the North American Great Plains, the relative abundance of *D. phi* sequences is less abundant than those of *D. alpha*. The functional role of *D. phi* on its host is unclear.

DISCUSSION

In the present study, we describe *D. phi*, sp. nov., a new species of *Darksidea* and its distribution, abundance, and host association in the North American Great Plains. The multigene phylogenetic analysis (FIG. 1) showed strong support for the placement of this novel species within the genus *Darksidea*, increasing the number of described congenerics to seven (Knapp et al. 2015). Eleven of 22 *Darksidea* isolates from grasses in North America were placed within *D. alpha*, five in *D. phi*, one in *D. zeta*, and five as *Darksidea* sp., showing great diversity of *Darksidea* species across North American grasslands (FIG. 1, TABLE 4). Similarly to other Pleosporalean fungi, single-locus analysis for the identification of *Darksidea* is unlikely to be sufficient for species or order resolution (Zhang et al. 2012). A previous study with multigene analyses resolved *Darksidea* placement in the Pleosporales order, in the Lentitheciaceae family, and strongly identified six *Darksidea* species using multigene analysis (Knapp et al. 2015).

Here, we provide the first genome of *D. phi*, a root colonizer of grasslands. To date, only the genomes of a few root endophytes are available, including *Cadophora, Periconia macrospinosa*, and *D. alpha* (Knapp et al. 2018). The availability of the *D. phi* genome can be used for comparative analysis to better understand their role in grasses and lifestyle, for the identification of annotated genes and proteins of interest, and for a comprehensive description of evolutionary relationships between different species.

Similar to other *Darksidea* species (Knapp et al. 2015), *D. phi* culture morphology was variable on different media (FIG. 2). Colonies of all described *Darksidea* species share characteristics with isolates of *D. phi*. For example, brown and olivaceous gray colonies were common in all

previously described *Darksidea* species (Knapp et al. 2015). Some isolates of *D. alpha* also grew in concentric circles (Knapp et al. 2015) (FIG. 2), and isolates of *D. phi* produced flat mycelium with some aerial mycelium—a universal *Darksidea* species characteristic (Knapp et al. 2015). DS919, DS697, and DS925 exuded metabolites in several media (FIG. 2). The chemical composition of these metabolites is not known; however, they are also common in other *Darksidea* species (Knapp et al. 2015). Slow- and fast-growing *D. alpha* isolates have also been identified by Knapp et al. (2015).

As with the shared colony characteristics, microscopic traits of *Darksidea* were similar to those described for other species in Pleosporales and in the genus *Darksidea*. Changes in hyphal pigmentation have been observed in other Pleosporales (Zhang et al. 2012). Anastomosis and branched hyphae of *D. phi* (FIG. 3, SUPPLEMENTARY FIG. 1) were common for several *Darksidea* species and other members of Lentitheciaceae, including *Kleissleriella aesculi* and *Leptosphaeria doliolum* (Zhang et al. 2012). Chlamydospores and hyphal coils that *D. phi* frequently develop have also been observed in *Allewia proteae* (Simmons 1990) and *Lewia chlamidosporiformans* (Vieira and Barreto 2010). However, production of chlamydospores, hyphal coils, and vesicle-like structures has not been reported for other *Darksidea* species. In contrast to other *Darksidea* species (Knapp et al. 2015), *D. phi* isolates did not develop ascomata, asci, or ascospores in any of the media we tested.

In our Illumina sequence data set, *D. alpha* was approximately 155 times more abundant across the 24 sites surveyed compared with *D. phi*. The high relative abundance of *D. alpha* is consistent with a previous report (Knapp et al. 2015). For example, 23 out of 33 isolates recovered from the Great Hungarian Plain were identified as *D. alpha* (Knapp et al. 2015). *Darksidea zeta* also occurred at low abundance at these sites in Hungary, represented by one isolate according to Knapp et al. (2015). Even though *D. phi* is closely related to *D. gamma* and *D. beta* (FIG. 1), no isolates or sequences of this taxon have yet been reported outside of North America (FIG. 1).

This new species was detected in culture-based and sequencing surveys (Lagueux et al. 2020; Porras-Alfaro et al. 2008, 2017). *Darksidea phi* sequences were highly abundant in the western sites at lower latitudes (FIG. 4). Similar patterns were identified for *D. alpha* by Rudgers et al. (2022). Southwestern sites are characterized by warmer temperatures and lower rainfall (227–551 Mean Annual Precipitation (MAP)) compared with the other sampled sites. The distribution and abundance of *D. phi* were consistent with reports for other *Darksidea* in roots, soils, and biocrusts of semiarid regions in the United States, Hungary, China, and Mongolia (Herrera et al. 2010; Knapp et al. 2019, 2015, 2012; Li et al. 2018; Porras-Alfaro et al. 2011, 2008). However, the distribution of this new species was not limited to semiarid regions; sequences and isolates of *D. phi* were also detected in cooler, mesic areas in Texas, Arkansas, and Kansas.

Similarly, *D. phi* was isolated from four of the five grass species in this study. Direct sequencing showed the highest abundance in *B. gracilis* and *B. eriopoda* compared with *B. dactyloides, A. gerardii*, and *S. scoparium* (FIG. 5). Internal transcribed spacer sequences that match *D. phi* have also been amplified from Canada (GQ923954) and from *Sporobolus cryptandrus* (HQ389481) in New Mexico (Herrera et al. 2010). Low host specificity has been also observed in other *Darksidea* species in associations with the Poaceae family (Herrera et al. 2010; Knapp et al. 2015; Porras-Alfaro et al. 2008). For example, *D. alpha* has been isolated from the same grasses as *D. phi* and also reported in *Festuca vaginata*. *Darksidea beta, D. gamma*, and *D. delta* have been reported in *F. vaginata; D. epsilon* from *F. vaginata* and *B. dactyloides*; and *D. zeta* from *Stipa borysenthica* and *B. gracilis* (Knapp et al. 2015).

Several geographic, abiotic, and climate factors, as well as plant traits, were predictors of *D. phi* relative abundance in semiarid grasses in the Great Plains in the United States. *Darksidea phi* sequence relative abundance was correlated to elevation (16%) and latitude (12%). Similarly, latitude and elevation have been identified as moderate correlates of fungal rhizobiome composition and DSF colonization in grasses (Lagueux et al. 2020; Ranelli et al. 2015; Rudgers et al. 2022). Furthermore, *D. phi* sequence relative abundance varied depending on the interactions of host plant species and latitude (FIG. 6). On *B. dactyloides, A. gerardii*, and *S. scoparium*, relative abundances of *D. phi* sequences decrease with rising latitude. Similarly to *D. phi*, pH, soil nitrogen, and soil phosphorus were identified as significant abiotic correlates of fungal rhizobiome composition on *A. gerardii, B. dactyloides, S. scoparium*, and other grasses (Ranelli et al. 2015; Rudgers et al. 2022). In addition to climate and edaphic factors, specific leaf area was a predictor of *D. phi* sequence relative abundance. Recent studies identified SLA as an important factor that regulates drought resistance in semiarid grasses (Lagueux et al. 2020)

Darksidea phi is distributed beyond the semiarid regions in the United States. The taxon has low host specificity among host grasses examined thus far and shows high variability in terms of morphological and microscopic structures. Further, both culture-based and direct Illumina sequencing approaches confirmed that this fungus is more abundant in the southwestern

United States, but the distribution extends into mesic tallgrass prairies across the North American Great Plains.

ACKNOWLEDGMENTS

Isolation of *Darksidea* cultures was possible due to sampling efforts and processing by Anny Chung, Terri Billingsley Tobias, Terry Torres-Cruz, Cedric Ndinga Muniania, Paris Salazar-Hamm, Shane Mason, and Adeyemi Olanrewaju. The authors would like to thank past and current members of the Fungal Ecology Laboratory at Western Illinois University for the help provided to process the samples.

DISCLOSURE STATEMENT

No potential conflict of interest was reported by the author(s).

FUNDING

The research presented in this paper was supported by NSF-DEB no. 1457309 to Dr. Jumpponen, no. 1619935 to Dr. Herrera, no. 1457002 to Dr. Porras-Alfaro, and no. 1456955 to Dr. Rudgers, and by the U.S. Department of Energy (DOE) Biological and Environmental Research Division through a Science Focus Area grant to Dr. Dunbar (F255LANL2018) and Dr. Cheryl Kuske (F260LANL2013). This research was partly supported by the National Research, Development and Innovation Office, Hungary (NKFIH KH-130401 and K-139026), the ELTE Thematic Excellence Program 2020 by National Research, Development and Innovation Office (TKP2020-IKA-05), and the János Bolyai Research Scholarship of the Hungarian Academy of Sciences to Dániel G. Knapp. This material is based upon work supported by the National Science Foundation (A.P.-A.). Any opinion, findings, and conclusions or recommendations expressed in this material are those of the author(s) and do not necessarily reflect the views of the National Science Foundation.

ORCID

María-José Romero-Jiménez http://orcid.org/0000-0003-3913-8907
Ari Jumpponen http://orcid.org/0000-0002-6770-2563
Miriam Hutchinson http://orcid.org/0000-0003-4077-0184
Dániel G. Knapp http://orcid.org/0000-0002-7568-238X
Andrea Porras-Alfaro http://orcid.org/0000-0002-9053-7973

LITERATURE CITED

Albright MB, Johansen R, Lopez D, Steven B, Kuske CR, Dunbar J. 2018. Short-term transcriptional response of microbial communities to nitrogen fertilization in a pine forest soil. Appl Environ Microbiol. 84:00598–18.

Andrews S. 2010. FastQC: a quality control tool for high throughput sequence data [cited April 2020]. http://www.bioinformatics.babraham.ac.uk/projects/fastqc

Bankevich A, et al. 2012. SPAdes: a new genome assembly algorithm and its applications to single-cell sequencing. J Comput Biol. 19:455–77.

Barton K. 2019. Mu-Min: multi-Model Inference. R-package version 1.43.15.

Bates D, Maechler M, Bolker B, Walker S. 2015. Fitting linear mixed-effects models using lme4. J Stat Softw. 67:1–48.

Berthelot C, Zegeye A, Gaber DA, Chalot M, Franken P, Kovács GM, Leyval C, Blaudez D. 2020. Unravelling the role of melanin in Cd and Zn tolerance and accumulation of three dark septate endophytic species. Microorganisms. 8:537.

Bokati D, Herrera J, Poudel R. 2016. Soil influences colonization of root-associated fungal endophyte communities of maize, wheat, and their progenitors. J Mycol. 2016:8062073.

Borchsenius F. 2009. FastGap 1.2. Software distributed by the authors. [accessed 2020 May 18]. http://www.aubot.dk/FastGap_home.htm

Bushnell B, Rood J, Singer E. 2017. BBMerge–accurate paired shotgun read merging via overlap. PloS ONE. 12:e0185056.

Carbone I, Kohn LM. 1999. A method for designing primer sets for speciation studies in filamentous ascomycetes. Mycologia. 91:553–56.

Cole JR, Wang Q, Fish JA, Chai B, McGarrell DM, Sun Y, Brown CT, Porras-Alfaro A, Kuske CR, and Tiedje JM. 2014. Ribosomal Database Project: Data and Tools for High Throughput rRNA Analysis. Nucleic Acids Research. 41:1–10.

Dayarathne MC, Wanasinghe DN, Jones EBG, Chomnunti P, Hyde KD. 2018. A novel marine genus, *Halobyssothecium* (Lentitheciaceae) and epitypification of *Halobyssothecium obiones* comb. nov. Mycol Prog. 17:1161–71.

Gaber DA, Berthelot C, Camehl I, Kovács GM, Blaudez D, Franken P. 2020. Salt stress tolerance of dark septate endophytes is independent of melanin accumulation. Front Microbiol. 11:3158.

Gardes M, Bruns TD. 1993. ITS primers with enhanced specificity for basidiomycetes - application to the identification of mycorrhizae and rusts. Mol Ecol. 2:113–18.

Glass NL, Donaldson G. 1995. Development of primer sets designed for use with PCR to amplify conserved genes from filamentous ascomycetes. Appl Environ Microbiol. 61:1323–30.

Groenewald JZ, Nakashima C, Nishikawa J, Shin HD, Park JH, Jama AN, Groenewald M, Braun U, Crous PW. 2013. Species concepts in *Cercospora*: spotting the weeds among the roses. Stud Mycol. 75:115–70.

Gurevich A, Saveliev V, Vyahhi N, Tesler G. 2013. QUAST: quality assessment tool for genome assemblies. Bioinformatics. 29:1072–75.

Haridas S, et al. 2020. 101 Dothideomycetes genomes: a test case for predicting lifestyles and emergence of pathogens. Stud Mycol. 96:141–53.

Haselwandter K, Read DJ. 1982. The significance of a root-fungus association in two *Carex* species of high-alpine plant communities. Oecologia. 53:352–54.

Herrera J, Khidir H, Eudy D, Porras-Alfaro A, Natvig D, Sinsabaugh R. 2010. Shifting fungal endophyte communities colonize *Bouteloua gracilis*: effect of host tissue and geographical distribution. Mycologia. 102:1012–26.

Ihrmark K, et al. 2012. New primers to amplify the fungal ITS2 region - evaluation by 454-sequencing of artificial and natural communities. FEMS Microbiol Ecol. 82:666–77.

Jumpponen A, Herrera J, Porras-Alfaro Rudgers J. 2017. Biogeography of root-associated fungal endophytes. In: Tedersoo L, editor. Biogeography of Mycorrhizal Symbiosis. Tartu (Estonia): Springer Nature; p. 195–222.

Jumpponen A, Trappe JM. 1998. Dark septate endophytes: a review of facultative biotrophic root-colonizing fungi. New Phytol. 140:295–310.

Kahle D, Wickham H. 2013. ggmap: spatial Visualization with ggplot2. R J. 5:144–61.

Katoh K, Rozewicki J, Yamada KD. 2017. MAFFT online service: multiple sequence alignment, interactive sequence choice and visualization. Brief Bioinform. 20:1160–66.

Khidir H, Eudy D, Porras-Alfaro A, Herrera J, Natvig D, Sinsabaugh R. 2010. A general suite of fungal endophytes dominate the roots of two dominant grasses in a semiarid grassland. J Arid Environ. 74:35–42.

Knapp DG, et al. 2018. Comparative genomics provides insights into the lifestyle and reveals functional heterogeneity of dark septate endophytic fungi. Sci Rep. 8:6321.

Knapp DG, Imrefi I, Boldpurev E, Csíkos S, Berek-Nagy PJ, Akhmetova G, Otgonsuren B, Kovács GM. 2019. Root colonizing endophytic fungi of the dominant grass *Stipa kryloyii* from a Mogolian steppe grassland. Front Microbiol. 10:2565.

Knapp DG, Kovács GM, Zajta E, Groenewald JZ, Crous PW. 2015. Dark septate endophytic pleosporalean genera from semiarid areas. Persoonia. 35:87–100.

Knapp DG, Pintye A, Kovács GM. 2012. The dark side is not fastidious - dark septate endophytic fungi of native and invasive plants of semiarid sandy areas. PLoS ONE. 7: e32570.

Kumar S, Stecher G, Tamura K. 2016. MEGA7: molecular Evolutionary Genetics Analysis version 7.0 for bigger datasets. Mol Biol Evol. 33:1870–74.

Lady Bird Johnson Wildflower Center. 2009. *Bouteloua eriopoda*. Austin: The University of Texas at Austin; [accessed 2019 Oct 22]. https://www.wildflower.org/plants/result.php?id_plant=BOER4

Lady Bird Johnson Wildflower Center. 2012. *Bouteloua gracilis*. Austin: The University of Texas at Austin; [accessed 2019 Oct 22]. https://www.wildflower.org/plants/result.php?id_plant=bogr2

Lady Bird Johnson Wildflower Center. 2015. *Andropogon gerardii*. Austin: The University of Texas at Austin; [accessed 2019 Oct 22]. https://www.wildflower.org/plants/result.php?id_plant=ANGE

Lady Bird Johnson Wildflower Center. 2018. *Bouteloua dactyloides*. Austin: The University of Texas at Austin; [accessed 2019 Oct 22]. https://www.wildflower.org/plants/result.php?id_plant=BODA2

Lady Bird Johnson Wildflower Center. 2019. *Schizachyrium scoparium*. Austin: The University of Texas at Austin; [accessed 2019 Oct 22]. https://www.wildflower.org/plants/result.php?id_plant=SCSC

Lagueux D, Jumpponen A, Porras-Alfaro A, Herrera J, Chung YA, Baur LE, Smith MD, Knapp AK, Collins SL, Rudgers JA. 2020. Experimental drought re-ordered assemblages of root-associated fungi across North American grasslands. Br Ecol Soc. 103:776–92.

Li X, He X, Hou L, Ren Y, Wang S, Su F. 2018. Dark septate endophytes isolated from a xerophyte plant promote the growth of *Ammopiptanthus mongolicus* under drought conditions. Sci Rep. 8:7896.

Mandyam K, Jumpponen A. 2005. Seeking the elusive function of the root-colonising dark septate endophytic fungi. Stud Mycol. 53:173–89.

Mandyam K, Loughin T, Jumpponen A. 2010. Isolation and morphological and metabolic characterization of common endophytes in annually burned tallgrass prairie. Mycologia. 102:813–21.

Nagy LG, Kocsubé S, Csana Z, Kovács GM, Petkovits T, Vágvölgyi C, Papp T. 2012. Re-mind the gap! Insertion–deletion data reveal neglected phylogenetic potential of the nuclear ribosomal internal transcribed spacer (ITS) of fungi. PLoS ONE. 7:e49794.

Pereira E, Vázquez de Aldana BR, San Emeterio L, Zabalgogeazcoa I. 2019. A survey of culturable fungal endophytes from *Festuca rubra* subsp. *pruinosa*, a grass from marine cliffs, reveals a core microbiome. Front Microbiol. 9:3321.

Pintye A, Knapp DG. 2021. Two pleosporalean root-colonizing fungi, *Fuscosphaeria hungarica* gen. et sp. nov. and *Delitschia chaetomioides*, from a semiarid grassland in Hungary. Mycol Prog. 20:39–50.

Porras-Alfaro A, Bayman P. 2011. Hidden fungi, emergent properties: endophytes and microbiomes. Annu Rev Phytopathol. 49:291–315.

Porras-Alfaro A, Herrera J, Natvig D, Lipinski K, Sinsabaugh R. 2011. Diversity and distribution of soil fungal communities in a semiarid grassland. Mycologia. 103:10–21.

Porras-Alfaro A, Herrera J, Sinsabaugh R, Odenbach K, Lowrey T, Natvig D. 2008. Novel root fungal consortium associated with a dominant desert grass. Appl Environ Microbiol. 74:2805–13.

Porras-Alfaro A, Muniania-Nninga C, Hamm PS, Torres-Cruz TJ, Kuske CL. 2017. Fungal Diversity and Function in Desert Ecosystems. In: Steven B, editor. The Biology of Arid Soils Biology. New Haven (Connecticut): De Gruyter; p. 97–115.

Quaedvlieg W, Kema GHJ, Groenewald JZ, Verkley GJM, Seifbarghi S, Razavi M, Mirzadi-Gohari A, Mehrabi R, Crous PW. 2011. *Zymoseptoria* gen. nov.: a new genus to accommodate *Septoria*-like species occurring on graminicolous hosts. Persoonia. 26:57–69.

Ranelli LB, Hendricks WQ, Lynn JS, Kivlin SN, Rudgers JA. 2015. Biotic and abiotic predictors of fungal colonization in grasses of the Colorado Rockies. Divers Distrib. 21:962–76.

Redman R, Sheehan KB, Stout RG, Rodriguez RJ, Henson JM. 2002. Thermo tolerance generated by plant/fungal symbiosis. Science. 298:1581.

Riddell WD. 1950. Permanent stained mycological preparations obtained by slide culture. Mycologia. 42:265–70.

Ronquist F, Huelsenbeck JP. 2003. MRBAYES 3: bayesian phylogenetic inference under mixed models. Bioinformatics. 19:1572–74.

Ronquist F, Teslenko M, van der Mark P, Ayres DL, Darling A, Höhna S, Larget B, Liu L, Suchard MA, Huelsenbeck JP. 2012. MRBAYES 3.2: efficient Bayesian phylogenetic inference and model selection across a large model space. Syst Biol. 61:539–42.

Rudgers JA, Fox S, Porras-Alfaro A, Herrera J, Kent D, Souza L, Chung YA, Jumpponen A. 2021. Data from: biogeography of root fungi in grasslands ver 2 [dataset]. Environ Data Initiative. Sept 30. accessed 2021 Nov 22. doi:10.6073/pasta/3f63cf15ed0851494a79ba13761cd236.

Rudgers JA, Fox S, Porras-Alfaro A, Herrera J, Reazin C, Kent DR, Souza L, Chung A, Jumpponen A. 2022. Biogeography of root-associated fungi in foundation grasses of North American Plains. J Biogeogr. 49:22–37.

Schoch CL, Seifert KA, Huhndorf S, Robert V, Spouge JL, Levesque CA, Chen W; Fungal Barcoding Consortium. 2012. Nuclear ribosomal internal transcribed spacer (ITS) region as a universal DNA barcode marker for Fungi. Proc Natl Acad Sci U S A. 109:6241–46.

Silvestro D, Michalak I. 2012. raxmlGUI: a graphical frontend for RAxML. Org Divers Evol. 12:335–37.

Simão FA, Waterhouse RM, Ioannidis P, Kriventseva EV, Zdobnov EM. 2015. BUSCO: assessing genome assembly and annotation completeness with single-copy orthologs. Bioinformatics. 31:3210–12.

Simmons EG. 1990. *Embellisia* and related teleomorphs. Mycotaxon. 38:251–65.

Simmons MP, Ochoterena H, Carr TG. 2001. Incorporation, relative homoplasy, and effect of gap characters in sequence based phylogenetic analysis. Syst Biol. 50:454–62.

Stamatakis A. 2014. RAxML version 8: a tool for phylogenetic analysis and post-analysis of large phylogenies. Bioinformatics. 30:1312–13.

Stanke M, Steinkamp R, Waack S, Morgenstern B. 2004. AUGUSTUS: a web server for gene finding in eukaryotes. Nucleic Acids Res. 32:309–12.

Tanaka K, Hirayama K, Yonezawa H, Sato G, Toriyabe A, Kudo H, Hashimoto A, Matsumura M, Harada Y, Kurihara Y. 2015. Revision of the Massarineae (Pleosporales, Dothideomycetes). Stud Mycol. 82:75–136.

Vieira B, Barreto R. 2010. Liquid culture production of chlamydospores of *Lewia chlamidosporiformans* (Ascomycota: pleosporales), a mycoherbicide candidate for wild poinsettia. Australas Plant Pathol. 39:154–60.

White TJ, Bruns T, Lee S, Taylor JW. 1990. Amplification and direct sequencing of fungal ribosomal RNA genes for phylogenetics. In: Innis MA, Gelfand DH, Sninsky JJ, White TJ, editors. PCR protocols: a guide to methods and applications. New York, NY: Academic Press; p. 315–22.

Wickham H. 2016. ggplot 2: elegant graphics for data analysis. New York (New York): Springer-Verlag.

Xu L, Bao D-F, Luo Z-L, Su X-J, Shen H-W, Su H-Y. 2020. Lignicolous freshwater ascomycota from Thailand: phylogenetic and morphological characterisation of two new freshwater fungi: *tingoldiago hydei* sp. nov. and *T. clavata* sp. nov. from Eastern Thailand. MycoKeys. 65:119–38.

Young ND, Healy J. 2003. GapCoder automates the use of indel characters in phylogenetic analysis. BMC Bioinform. 4:6.

Zhang Y, Crous P, Schoch C, Hyde K. 2012. Pleosporales. Fungal Divers. 53:1–221.